

# Robustness of the Brain Parenchymal Fraction for Measuring Brain Atrophy

M. Stella Atkins, Jeff J. Orchard, Ben Law, Melanie K. Tory  
School of Computing Science, Simon Fraser University, Burnaby, B.C., Canada, V5A 1S6

## ABSTRACT

Other researchers have proposed that the brain parenchymal fraction (or brain atrophy) may be a good surrogate measure for disease progression in patients with Multiple Sclerosis. This paper considers various factors influencing the measure of the brain parenchymal fraction obtained from dual spin-echo PD and T2-weighted head MRI scans. We investigate the robustness of the brain parenchymal fraction with respect to two factors: brain-mask border placement which determines the brain intra-dural volume, and brain scan incompleteness.

We show that an automatic method for brain segmentation produces an atrophy measure which is fairly sensitive to the brain-mask placement. We also show that a robust, reproducible brain atrophy measure can be obtained from incomplete brain scans, using data in a centrally placed subvolume of the brain.

Keywords: Brain atrophy, brain parenchymal fraction, brain segmentation sensitivity

## 1 INTRODUCTION

Measures of brain atrophy may be used to monitor degenerative conditions such as Multiple Sclerosis (MS) [1,2,3,4]. A reliable measure of brain atrophy is the brain parenchymal fraction (BPF)[2,3,5], calculated from the intra-dural volume (IDV) and the volume of the cerebral-spinal fluid (CSF) using the formula  $BPF = (IDV - CSF) / IDV$ . A decrease in BPF over time might give early diagnostic clues about the onset of MS [2].

The sensitivity of the BPF to processing parameters is not fully understood. Some studies have made observations about BPF behavior [5,6,7]. For example, slight changes in the segmentation of CSF can influence the BPF dramatically. However, automatic segmentation of the CSF yields BPF time-series behavior that is highly reproducible [6].

With the onset of better automatic brain segmentation methods, we wish to study the behavior of the BPF with respect to subtle differences in the brain-mask border. Furthermore, full-brain datasets are not always available for analysis. It is unclear how this incompleteness affects the calculation of the BPF, and whether or not a meaningful BPF trend can accurately be determined despite it. In this paper, we investigate the sensitivity of the BPF with respect to two factors: brain-mask border placement, and brain scan incompleteness.

## 2 MATERIALS AND METHODS

The data consists of two sets from different MS patients, labeled A and B, of dual spin-echo PD and T2 scans axially acquired for MS studies with  $TR = 3000\text{ms}$ ,  $TE = 30\text{ms}$  and  $90\text{ms}$ , slice thickness =  $5\text{mm}$ , and in-plane pixel size of  $0.859\text{mm}^2$ . The datasets A and B contain a time-series of 11 and 8 brain scans respectively, taken roughly one scan every month. Set A with 22 slices is an incomplete brain volume, missing the top 2 slices. Set B contains the complete brain, in 24 slices.

The brain atrophy measures are based on our automatic method for segmenting the brain from the head in MRI scans [8,10]. As a preprocessing step for every volume, the intensity values are normalized by remapping the voxel intensities within 3 standard deviations from the mean to the range  $[0, 255]$  (detailed in [9]). To segment the CSF from the normalized brain images, we calculated the ratio image, PD/T2, and applied a threshold to extract the CSF, as described in the first step of our automatic method for isolating MS lesions [10]. In the ratio image, the CSF appeared dark since the CSF is very bright in T2-weighted MR images.

The brain mask was obtained by anisotropic diffusion of the T2 image, followed by thresholding the resulting blurry image, according to [8,10]. The non-brain areas, such as the eyes, were removed by morphological operations. Finally, the initial mask was refined using the "snakes" algorithm. The intra-dural volume (IDV) was obtained from this mask.

We tested the sensitivity of the BPF measurements with respect to two major parameters: the outline of the intra-dural brain mask, and the subvolume of the brain used in the calculation. The IDV depends on the brain mask, so measures of the IDV alone would require very accurate thresholding of the head image. Our automatic method is 100% reproducible, and has been assessed to be acceptably accurate [8]. However, absolute measures of the IDV are dependent on partial volume effects, especially for thick slices. The sensitivity of the IDV (and hence the BPF) to the brain mask border was measured by applying morphological image erosion and dilation to the original brain mask for dataset B. Square kernels of 3x3 and 5x5 were used for both erosion and dilation to produce alternative brain masks. These new masks were used for preprocessing and renormalization of the data prior to obtaining the IDV, CSF and BPF.

To simulate incomplete brain scans, we examined various brain subvolumes to evaluate how well their temporal BPF behavior correlated with that of the entire scan. Various subsets of the slices were considered, including every second and every third slice. However, our study focussed mainly on subvolumes of sequential slices. We selected a subvolume by placing a sliding window over a subset of the slices. The BPF analysis continued as though the selected slices were the only ones acquired in the dataset. Hence, the subvolume BPF was calculated by finding the total IDV and total CSF of the windowed slices. In this manner, a subvolume BPF time-series was generated for both dataset A and dataset B.

By shifting the sliding window, a different subvolume is created. BPF time-series were generated by centering the sliding window on the ventricles, and then offsetting the window by single-slice increments in both the inferior and superior directions. Thus, for every sliding window offset, a time-series of BPF values can be compared to the BPF time-series of the full volume. Of interest here is the degree to which the trends in the subvolume BPF follow those of the entire volume. Each resulting BPF time-series was compared to the full-scan BPF time-series by calculating their correlation coefficient.

### 3 RESULTS

#### 3.1 Intra-Dural Volume

The time series of intra-dural volumes for datasets A and B, obtained by automatic segmentation from the head, are plotted in Figure 1. For patient A, the mean IDV = 1263.2mL, standard deviation  $\sigma = 14.49\text{mL}$ , and the coefficient of variation (CV)= 1.15%. For patient B, the mean IDV = 1117.7mL, standard deviation  $\sigma = 3.06\text{mL}$ , and the CV = 0.27%.

The brain parenchymal fraction time-series for each dataset is plotted in Figure 2. For dataset A, the mean BPF = 0.829, standard deviation  $\sigma = 0.0048$  (assuming no trend) and the CV = 0.584%. Regression analysis shows a significant downward trend of -0.00148 per time unit ( $R^2 = 90.7\%$ , significance  $F < 0.00001$ ). For patient B, the mean BPF = 0.838, standard deviation  $\sigma = 0.0031$ , and the CV = 0.369%. This patient shows a smaller, insignificant downward trend ( $R^2 = 17\%$ ; significance  $F = 0.3$ ).

#### 3.2 Brain Mask Erosion and Dilation

Figure 3 shows the effect on the BPF of changes to the brain mask for dataset B, through erosion and dilation of the original brain masks. The BPF results calculated using a 3x3 erosion kernel over the brain mask for patient B (mean BPF=0.838) are almost identical to the BPF values calculated from the non-dilated mask (mean BPF=0.837). The other eroded/dilated brain masks yield slightly elevated BPF values, with mean values greater than 0.843. For any given scan in dataset B, the standard deviation of the BPF measurements among the eroded, dilated, and original brain masks was higher than 0.45%. The original full-scan BPF time-series exhibited a standard deviation of only 0.31%.

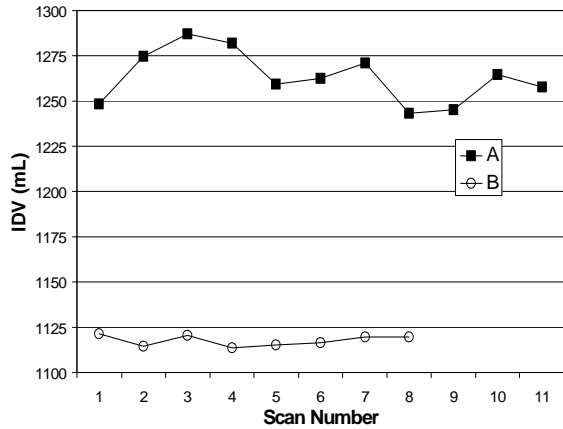


Figure 1. Intra-dural volume for the two datasets over time.

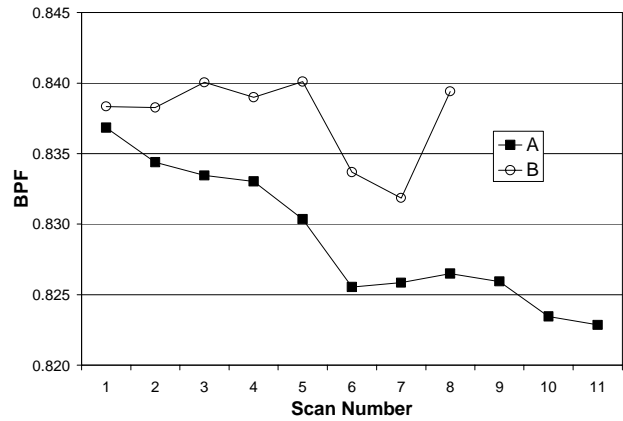


Figure 2. BPF for the two datasets over time.

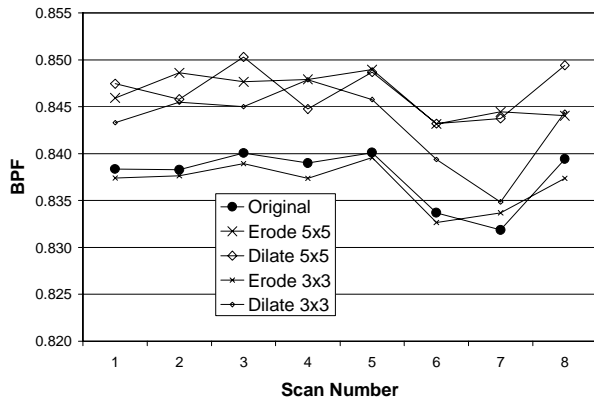


Figure 3. Effect of erosion and dilation of brain mask on BPF. Results are plotted for dataset B only. The 3x3 eroded BPF results are similar to the original, but all others have slightly increased BPF values.

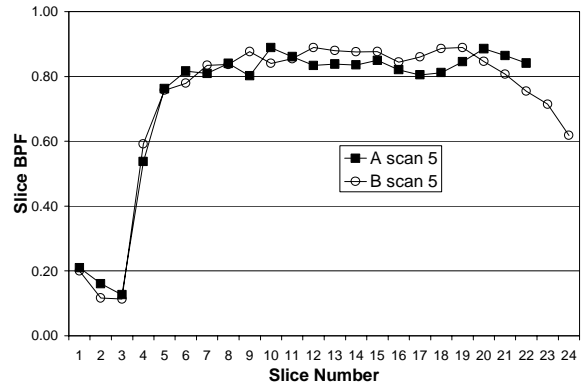


Figure 4. Slice BPF for scan number 5 of each dataset. The BPF of a given slice is calculated using the IDV and CSF from that slice only.

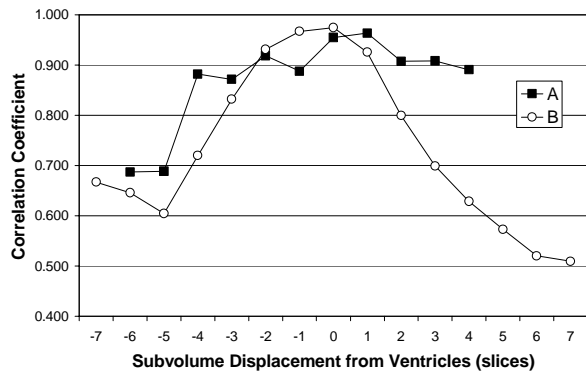


Figure 5. Correlation of subvolume and full-brain BPF time-series. For dataset A, 9 sequential slices were used. For dataset B, 7 sequential slices were used. The number of slices was chosen to match the span of the ventricles in each dataset. The x-axis shows the displacement of the subvolume's center slice from the ventricle's center slice (positive values represent superior placement). The maximum of each curve occurs near zero displacement, when the subvolume is approximately centered on the ventricles.

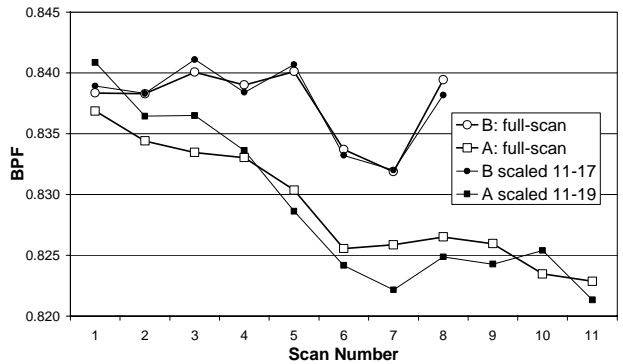


Figure 6. Scaled subvolume BPF time series and the full-scan BPF time-series. For dataset A, slices 10 to 18 are used. For dataset B, slices 11-17 are used. The subvolume BPF graphs were multiplied by a constant scale factor to minimize their mean squared error from the full-scan BPF.

### 3.3 Sub-volumes for BPF

Figure 4 shows how the BPF varies across the axial brain slices, from the bottom to the top, for a typical scan (scan 5 of each dataset).

To locate suitable sequential slices for subvolume BPF calculations, the slices were chosen by visual inspection to roughly match the number of slices containing the ventricles. Thus, for dataset A, each subvolume contained a window of 9 sequential slices, and for dataset B, each subvolume contained a window of 7 sequential slices. Figure 5 shows the correlation of various subvolume BPF time-series (generated from slices under the sliding window) with the full-brain BPF time series. The subvolume windows were centered on the ventricles, and offset by single-slice increments in both the inferior and superior directions. For each window offset, the resulting BPF time-series was compared to the full-brain BPF time-series using the cross-correlation measure.

Figure 6 plots the BPF for each scan of data sets A and B of the sub-volume centered on the ventricles, against the original BPF. Note that the sub-volume BPF graphs were multiplied by a constant scale factor to minimize their mean squared error.

## 4 DISCUSSION

### 4.1 Intra-dural Volume and Accuracy of Original BPF

We would expect a healthy patient's IDV to be nearly constant. The relatively large variation in brain volume recorded for patient A (see Figure 1) is likely due to the fact that the top 2 slices of the brain are not included in these datasets. The data therefore varies according to the position of the patient in the scanner. Dataset B has the complete brain imaged, and shows a much lower coefficient of variation for the IDV (1.15% for A, and 0.27 % for B).

Most researchers do not report the scan-rescan reproducibility of the intra-dural *volume* measurement, focusing instead on the *fraction* of brain in the observed measurements. Chen has reported scan-rescan reproducibility of two brain volume measurements on two volunteers, where the data was acquired with 1.5mm thick slices [4]. In one of these cases the difference between two scans was 0.6%. However, segmenting MR head images with 5mm thick slices is notoriously subject to partial volume effects, so our results for patient B are entirely reasonable.

For patient A, the CV of the BPF measurement is 0.584%. Note that this data set does not include the whole brain; the mis-registration of patient position causes a higher variance than would be observed for a whole brain BPF measurement. Indeed, for patient B, where the whole brain set is available, the CV is lower, at 0.369%. This is still higher than others have reported for scan-rescan measurements of BPF: Fisher reports a mean CV of 0.19% for the BPF from scan-rescan tests with 12 people, using T2-weighted FLAIR scans with 5mm thick slices [9] and Collins reports a mean CV of 0.21% on scan-rescan tests of 4 normal controls, using 3mm slices [10]. However, our results are not directly comparable, because we did not acquire scan-rescan images within a short time period. We expect some atrophy in MS patients to occur over time; Rudick reports a drop of 0.7% per year in placebo patients [2], Jones reports a drop of 0.84% [3], and Collins reports a drop of 1.8% for relapsing/remitting MS patients [10]. Our patient A shows a drop of 1.6% over the whole time series of 11 months, consistent with these findings.

### 4.2 Sensitivity of BPF to Brain Mask

Figure 3 shows the complicated interplay between the competing effects of subtle changes in the edges of the brain mask. Erosion tends to decrease CSF, which in turn increases BPF. However, erosion also decreases IDV, which has a decreasing effect on BPF. A similar statement can be made about dilation. Ultimately, the issue is the fraction of eroded/dilated tissue that is classified as CSF, and how that fraction compares to that fraction of the entire brain. Here, the observed variation in BPF due to subtle brain mask changes is greater than the variation in the BPF time-series itself. While it is encouraging to see that the BPF is almost unchanged when the initial brain mask is slightly eroded (3x3), most morphological operations on the brain mask induced a significant change in the BPF. This might suggest that it is prudent to err on the side of a slightly small brain mask rather than one that is larger. However, the results point out the sensitivity of BPF to small changes in the brain mask boundaries.

### 4.3 Sensitivity of BPF to sub-brain Volume

For axial scans, Figure 4 shows that the lower slices containing the brain stem have at most 20% white/grey matter, rising to nearly 90% in slices near the center not containing the ventricles. Note that data set A does not contain the full brain; the top few slices are missing. Therefore, only dataset B shows how the BPF is lowered in the top part of the brain, indicating that the proportion of CSF is higher in the topmost brain slices. From this figure, it can be seen that the range of slices from 6 to 21 exhibits a fairly constant BPF value. Hence, errors caused by patient misalignment will have a minimal effect on the BPF of a subvolume centered on these slices.

Figure 5 shows that the subvolume that included the slices through the ventricles yielded the lowest mean square error for comparable sub-volumes for both datasets, as the maximum of each curve occurs near zero displacement, when the sub-volume is approximately centered on the ventricles. Figure 6 shows that the subvolumes centered on the ventricles exhibit a temporal BPF trend very similar to that of the full-scan BPF.

## 5 CONCLUSIONS AND FUTURE WORK

We found that for purposes of measuring changes of the BPF over time in a particular patient, the BPF obtained automatically by our image processing techniques does indeed appear to be robust and reproducible. However, the variation in BPF among the eroded and dilated brain masks is much higher than the variation exhibited by the BPF time-series from the original brain mask. This effect illustrates the critical importance of the reproducibility and accuracy of brain segmentation. Variation in BPF due to inconsistent or inaccurate segmentation can overwhelm the variation in BPF due to brain atrophy.

The BPF of the axial slices through the ventricles follow a similar temporal trend to that of the full-scan BPF. This finding suggests that ventricular slices alone might be sufficient to reliably detect brain atrophy.

Future work will include many more patient and normal studies to confirm the sensitivity of the method. We then plan to use the method to determine brain atrophy trends in degenerative neural diseases such as MS and Alzheimer's disease.

## 6 ACKNOWLEDGMENTS

Many thanks to Dr. David Li for interesting discussions and advice, and to the UBC Multiple Sclerosis Group for providing the data. Funding was provided by the Canada Natural Science and Engineering Research Council.

## 7 REFERENCES

- [1] Simon, J.H. et al. "A longitudinal study of brain atrophy in relapsing Multiple Sclerosis", *Neurology*, 53(8), pp.139-148, July 1999.
- [2] Rudick, R.A. et al. "Use of the brain parenchymal fraction to measure whole brain atrophy in relapsing-remitting MS", *Neurology*, 53(8), pp.1698-1999, Nov. 1999.
- [3] Jones, C. et al., "Atrophy Measurements in Multiple Sclerosis", *Proceedings of ISMRM*, (9), page 1414, April 2001.
- [4] Chen D. et al. "A new method for quantitative analysis of Multiple Sclerosis using MR images", *Proceedings of SPIE Medical Imaging*, (4319), pp. 375-380, Feb. 2001.
- [5] Collins D.L. et al., "Automated estimation of brain volume in MS with BICCR", *Information Processing in Medical Imaging*, Springer-Verlag Lecture Notes in Computer Science, (2082), pp. 451-456, June 2001.
- [6] Atkins, M.S., Orchard, J., Tory, M.K., "Evaluation of Brain Atrophy Measures in MRI", *Proceedings of 23<sup>rd</sup> IEEE EMBS Conference*, Oct. 2001
- [7] Fisher, E. et al., "Automated Calculation of Whole Brain Atrophy from Magnetic Resonance Images for Monitoring Multiple Sclerosis", *Neurology*, (52): A352, 1999.
- [8] Atkins, M.S. and Mackiewicz, Blair T., "Fully Automatic Segmentation of the Brain in MRI", *IEEE Trans. on Medical Imaging*. 17(1), pp. 98-107, Feb. 1998.
- [9] Krishnan, K. and Atkins, M.S., "Segmentation of Multiple Sclerosis Lesions in MRI – An Image Analysis Approach", *Proceedings of SPIE Medical Imaging*, (3338), pp. 1106-1116, Feb. 1998.
- [10] Atkins, M.S. and Mackiewicz, Blair T., "Fully Automatic Hybrid Segmentation of the Brain", Bankman., ed., *Handbook of Medical Imaging*, Academic Press: San Diego, California, Chapter 11, pp. 171-183, 2000